



**Discover Generics**

Cost-Effective CT & MRI Contrast Agents



**FRESENIUS  
KABI**

[WATCH VIDEO](#)

**AJNR**

## **Pediatric Head CT: Automated Quantitative Analysis with Quantile Regression**




K.A. Cauley, Y. Hu and S.W. Fielden

*AJNR Am J Neuroradiol* published online 10 December 2020

<http://www.ajnr.org/content/early/2020/12/10/ajnr.A6885>

This information is current as of June 14, 2025.

# Pediatric Head CT: Automated Quantitative Analysis with Quantile Regression

 K.A. Cauley,  Y. Hu, and  S.W. Fielden



## ABSTRACT

**BACKGROUND AND PURPOSE:** Together with quantile regression methods, such a model would have the potential for clinical utility through automated quantitative comparison of individual cases relative to their age and gender-matched peer group. Our aim was to demonstrate the automated processing of digital clinical head CT data in the development of a clinically useful model of age-related changes of the brain in the first 2 decades of life.

**MATERIALS AND METHODS:** A total of 415 (209 female) consecutive, clinical head CTs with radiographically normal findings from patients from birth through 20 years of age were retrospectively selected and subjected to automated segmentation. Brain volume, brain parenchymal fraction, brain radiodensity, and brain radiomass were assessed as a function of patient age. Statistical modeling and quantile regression were performed.

**RESULTS:** Brain volume increased from 400 cm<sup>3</sup> at birth to 1350 cm<sup>3</sup> at 20 years of age (>3-fold). Males had a slightly steeper growth trajectory than females, with approximately 8% difference in volume between the sexes established in the first few years of life. Brain parenchymal fraction was variable at younger than 2 years of age, stabilizing between 0.85 and 0.92 at 2–3 years of age. Brain mean radiodensity was lower at birth (24 HU) and increased through 3 years of age, after which it stabilized near 30 HU, an approximately 25% increase. The product of brain volume and mean brain radiodensity (radiomass), increased from 700 HU × mL at birth to 3900 HU × mL, a 5.6-fold increase, with approximately 5% difference between males and females at 20 years. Quantile regression enables a given metric to be interpreted relative to an age- and sex-matched peer group.

**CONCLUSIONS:** Automated segmentation of clinical head CT images permitted the generation of a reference database for quantitative analysis of pediatric and adolescent brains. Quantile regression facilitates clinical application.

**ABBREVIATION:** BPF = brain parenchymal fraction

*“... it became apparent that the conventional methods were not making full use of all the information the X-rays could give.”*

*G. Hounsfield, Nobel Lecture, 1979*

**C**T is a highly calibrated and scaled imaging technique capable of volumetric and radiodensity assessment, though this capability is rarely used in the clinical setting. Concerns over

radiation exposure have limited prospective human subject research in CT and consequently have limited the investigation into the value of quantitative CT. Recent improvements in image quality and the availability of postprocessing software enable the generation of large reference databases from the existing clinical archives. Such databases facilitate research into quantitative CT by helping define the normal statistical variance, identify outliers, and correlate measurements with pathology.

In neuroimaging, brain volumetrics can have diagnostic value, as illustrated by prospective MR imaging studies of neurodegenerative diseases such as age-related dementia,<sup>1</sup> amyotrophic lateral sclerosis,<sup>2</sup> and multiple sclerosis.<sup>3,4</sup> The volumetrics of CT imaging data have been less extensively researched, though a recent study of automated segmentation of clinical head CT data shows that the brain volume is statistically smaller in patients with Alzheimer disease.<sup>5</sup> CT has the additional capability of voxel-based assessment of radiodensity, expressed in terms of Hounsfield units, a tissue

Received May 18, 2020; accepted after revision September 4.

From the Departments of Radiology (K.A.C.) and Biomedical and Translational Informatics (Y.H.), Geisinger Medical Center, Danville, Pennsylvania; and Geisinger Autism and Developmental Medicine Institute (S.W.F.), Lewisburg, Pennsylvania.

This work was funded by the Geisinger Clinical Research Fund to K.A.C. and S.W.F. (SRC-L-58).

Please address correspondence to Keith A. Cauley, MD, PhD, Geisinger Medical Center, Department of Radiology 100 N Academy Ave, Danville, PA 17822; e-mail: keithcauley@hotmail.com



Indicates article with supplemental online tables.



Indicates article with supplemental online photos.

<http://dx.doi.org/10.3174/ajnr.A6885>

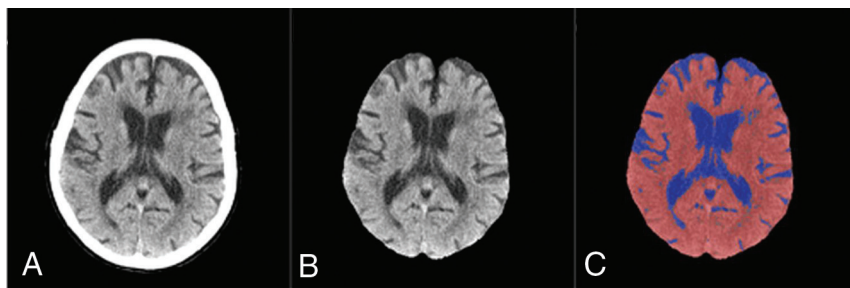


**FIG 1.** Products of automated head CT segmentation. Routine clinical head CT (A), brain-extracted image (B), and CSF eliminated (brain parenchyma) (C).

property measure that is unique to this technique. Because most brain imaging research has been conducted using MR imaging, there is little information on the diagnostic value of the brain radiodensity measure. It is well-established that mean brain radiodensity is abnormal in hypoxic-ischemic encephalopathy, for example, and quantitative assessment appears to have diagnostic and prognostic implications.<sup>6-8</sup> Mean brain radiodensity is also abnormal in multiple sclerosis,<sup>9</sup> and mean brain radiodensity shows a statistically significant decline as a function of aging.<sup>10</sup> It would, therefore, appear reasonable that other forms of encephalopathy or neurodegenerative disease may also demonstrate abnormalities of brain radiodensity, and radiodensity measures may serve to identify disease or quantify disease progression. As with brain volume measures, these types of studies will also require a reference normative data base.

In this study, we focus on the pediatric age group and apply an automated segmentation algorithm to a large number of retrospectively identified head CTs with radiographically normal clinical findings to initiate the development of a clinical reference data base for brain volume, parenchymal fraction, brain radiodensity, and brain radiomass. Such a data base can be subject to quantile regression analysis because individual cases can be referenced against their clinical peer group.

## MATERIALS AND METHODS

### Study Design

This study was limited to a retrospective analysis of head CTs performed on patients who were identified from the clinical PACS. The study was approved by this institutional review board (Geisinger Medical Center), and a waiver of consent was granted.

### Study Cohort

In total head CTs from 417 patients (209 females), 0–20 years of age, were included. Details regarding the imaging and data base for the neonates 0–2 years of age have been published previously.<sup>11</sup> The remaining cases were from a 2-year time interval (January 1, 2015, to December 31, 2016). Selected cases were scanned for trauma with no traumatic findings or nonspecific symptoms (headache, syncope, vertigo) without known systemic disease and were discharged without incident. All cases were interpreted as having normal findings (without acute or chronic abnormal findings) by 2 board-certified neuroradiologists. Patients older than 2 years of age were scanned in a single CT scanner (LightSpeed

VCT; GE Healthcare), which primarily serves the emergency department of a level 1 trauma center. The axial acquisition noncontrast head CT protocol was the following: 135kV(peak) and modulated milliampere, minimum 50 and maximum 290 mA, rotation time = 0.75 seconds, acquired from the foramen magnum through the vertex with a standard 512 × 512 matrix, 24-cm FOV at 5.0-mm section thickness. The scanner undergoes a daily quality-assurance procedure, which assesses the radiodensity of water. This value

must be within allowable limits, generally 0–5 HU. Drift or trending is rarely observed. In a typical month, the Hounsfield units of water or the tissue density plug is found to vary by <1 HU. In addition, scanners undergo an annual inspection by a medical physicist using the American College of Radiology phantom. Acceptable ranges of Hounsfield units for clinical scanners are broad (–7 to +7 for water, 110–135 for acrylic). This testing is extended to all kilovolt peaks used by the scanner. Additionally, service engineers routinely test the calibration at preventive maintenance.

### Image Processing and Analysis

DICOM images were converted to the Neuroimaging Informatics Technology Initiative (NIfTI; <https://nifti.nimh.nih.gov/>) data format using MRICConvert-2.0.7 (<http://lcn.uoregon.edu/jolinda/MRICConvert/>). Images were first thresholded from –15 to 50 HU to grossly remove background and skull. Brain extraction was then applied by using FSL Brain Extraction Tool (<http://fsl.fmrib.ox.ac.uk/fsl/fslwiki/BET>)<sup>12,13</sup> with a fractional intensity threshold of 0.01. All cases were carefully reviewed for integrity of brain extraction. For segmentation, FMRIB's Automated Segmentation Tool (FAST; <http://poc.vl-e.nl/distribution/manual/fsl-3.2/fast/index.html>) was used to generate a 3-tissue compartment segmentation with the resulting white matter and gray matter compartments combined into a single brain compartment (Fig 1). Brain radiomass was calculated as the product of mean brain radiodensity and total brain volume.

### Statistical Methods

Statistical analysis was performed using GraphPad Prism software, Version 7.0c for Mac OS X (GraphPad Software). Scatterplots were generated in Excel (Microsoft) for Mac 2011, Version 14.2.3.

The overall polynomial regression of age was fitted on brain volume and brain parenchymal fraction (BPF) to evaluate the impact of sex on the outcomes. When stratified by sex, quantile regression models with the polynomial term of age were adopted to characterize brain volume and BPF, respectively. A 2-phase model enabled the best fit of the data. A natural inflection at 2 years was confirmed by 2D cluster analysis using a Gaussian mixture model (Online Fig 1). The Gaussian mixture model is a probabilistic model that comprises Gaussian distributions. Each Gaussian in the mixture is represented by a mean and covariance matrix. For ages 0–2, the linear term of age was fit, where 0.05 and 0.10 quantiles were presented.

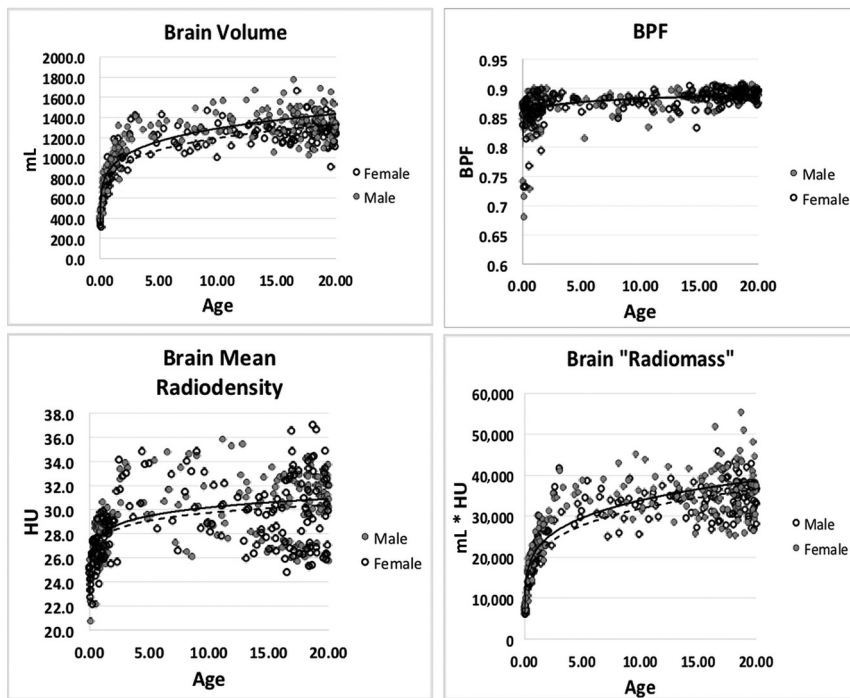


**FIG 2.** Scatterplots of computed brain metrics as a function of subject age: brain volume (A), BPF (B), mean brain radiodensity (C), and brain radiomass (D).

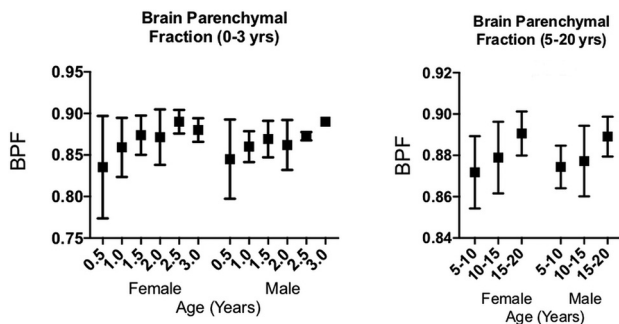


**FIG 3.** Box-and-whisker plots of BPF: 0–3 years (left) and 5–20 years (right). Tabular data below 0–3 years (Table 1). Data scatter is greater immediately after birth and decreases during the first 2 years, and the pattern is similar between the sexes. There is no significant difference between the mean BPF of the groupings. Table 2 shows statistically significant difference between the means of 5-year groupings.

**Table 1: Brain parenchymal fraction 0–3.0 years**

Age (yr)	Male			Female		
	Total	Mean	SD	Total	Mean	SD
0–0.5	20	0.845	0.047	17	0.84	0.062
0.5–1.0	15	0.86	0.018	23	0.86	0.035
1.0–1.5	12	0.87	0.022	13	0.87	0.024
1.5–2.0	10	0.86	0.030	7	0.87	0.033
2.0–2.5	4	0.87	0.005	2	0.89	0.014
2.5–3.0	2	0.89	0.000	4	0.88	0.014

For ages 2–20, a quadratic term of age was fit, in which 0.05 and 0.10 quantiles were presented. A *P* value of < .05 was considered statistically significant. Quantile regression models were performed in R Studio (Version 1.2.1335; <http://rstudio.org/download/desktop>). Quantile regression quadratic coefficients for 2–20 years of age are included in Online Tables 1–4.

## RESULTS

### Brain Volume

Brain volume (Fig 2A) increases from approximately 400 mL at birth to 1350 mL at 20 years of age; males had a slightly steeper growth trajectory than females, with approximately 8% difference in volume established in the first few years of life. For 0–2 years of age, males had higher mean brain volumes than females (mean difference = 37.94; 95% CI, 0.07–75.81; *P* = .05). For 2–20 years of age, males again had higher mean brain volumes than females (mean difference = 94.81; 95% CI, 69.53–120.09; *P* < .001).

### Brain Parenchymal Fraction

The BPF value was variable in subjects younger than 2 years of age, with lower numbers in the immediate postpartum period (Fig 3), after which it stabilized as a largely age- and sex-independent variable between 0.85 and 0.92 (Table 1 and Fig 2B). During adolescence, the slight increase in brain size is reflected in a small, gradual increase in BPF. The mean BPF at 5–10 years of age was 0.87, and at 15–20 years of age, it was 0.89, with differences being statistically significant (*P* < .001) and virtually identical between the sexes (Table 2 and Fig 2B).

### Brain Radiodensity

Brain tissue radiodensity was low at birth (mean, 24 HU) and increased through 3 years of age, after which it stabilized near 30 HU (Fig 2C). Although the data scatter is relatively large, there was no significant difference in mean density when comparing data between male and female cohorts. The mean radiodensity was not significantly changed among the age groups of 5–10, 10–15, and 15–20 years and was not significantly different between the sexes.

### Brain Radiomass

The product of brain volume and radiodensity (the radiomass) increased from 7000 HU × cm<sup>3</sup> at birth to 39,000 HU × cm<sup>3</sup>, a 5.6-fold increase, with an approximately 5% difference between males and females at 20 years of age (Fig 2D).

Direct comparison was made of changes in brain volume, brain radiodensity, and brain radiomass. Brain volume and brain

radiodensity increased along similar power trendlines in the first few years of life. Because the product of these 2 measures is the radiomass, we further investigated the correlation between these 2 variables by normalization and plotting on the same graph. When normalized for direct comparison, the radiodensity nearly plateaued at 3 years of age, whereas the volume continued to increase through early adulthood (Online Fig 2). The radiomass showed a small-but-consistent increase through adolescence and early adulthood. All 3 sets of curves are virtually identical between male and female patient groups. This high level of reproducibility between independent datasets (male and female patients) suggests that the trends are not significantly influenced by the presence of abnormal outliers and approximate normalcy.

**Table 2: Brain parenchymal fraction 5–20 years**

Age (yr)	Total	Mean	5–10 Years (P Value)	10–15 Years (P Value)
Male				
5–10	18	0.872		
10–15	20	0.879	NS	
15–20	72	0.891	<.001	.004
Female				
5–10	12	0.874		
10–15	20	0.877	NS	
15–20	70	0.889	.003	.003

**Note:**—NS indicates not significant.

## Quantile Regression

Quantile regression provides a means to compare individual cases with their age- and sex-matched clinical peer group. Quantile regression of brain volume and BPF is shown in Fig 4. A linear regression is a best fit for the 0–2 age group, and a polynomial best fit is used for the 2–20 years-of-age grouping; quadratic coefficients are shown in Online Tables 1–4.

## DISCUSSION

This study was motivated by a desire to bring quantitative methods to otherwise qualitative clinical head CT interpretation. The objectives of our study were the following: 1) to demonstrate automated data processing of clinical head CTs, 2) to demonstrate that these data can be used to develop a model of age-related changes in the first 2 decades of life that approaches normative data, and 3) to apply quantile regression methods to show how individual cases compare with their age- and sex-matched peer group.

### Potential Value of Quantitative CT

CT is a very widely used first-line clinical imaging technique, though quantitative brain CT imaging has received considerably less research attention than MR imaging. CT can generate volumetrics and radiodensity measures. We know from MR imaging that brain volume and BPF have clinical implications.<sup>1–4</sup> Because radiodensity is a measure that only CT can provide, there is currently little information regarding the use of the radiodensity measure to evaluate global brain parenchyma. It is well-established that

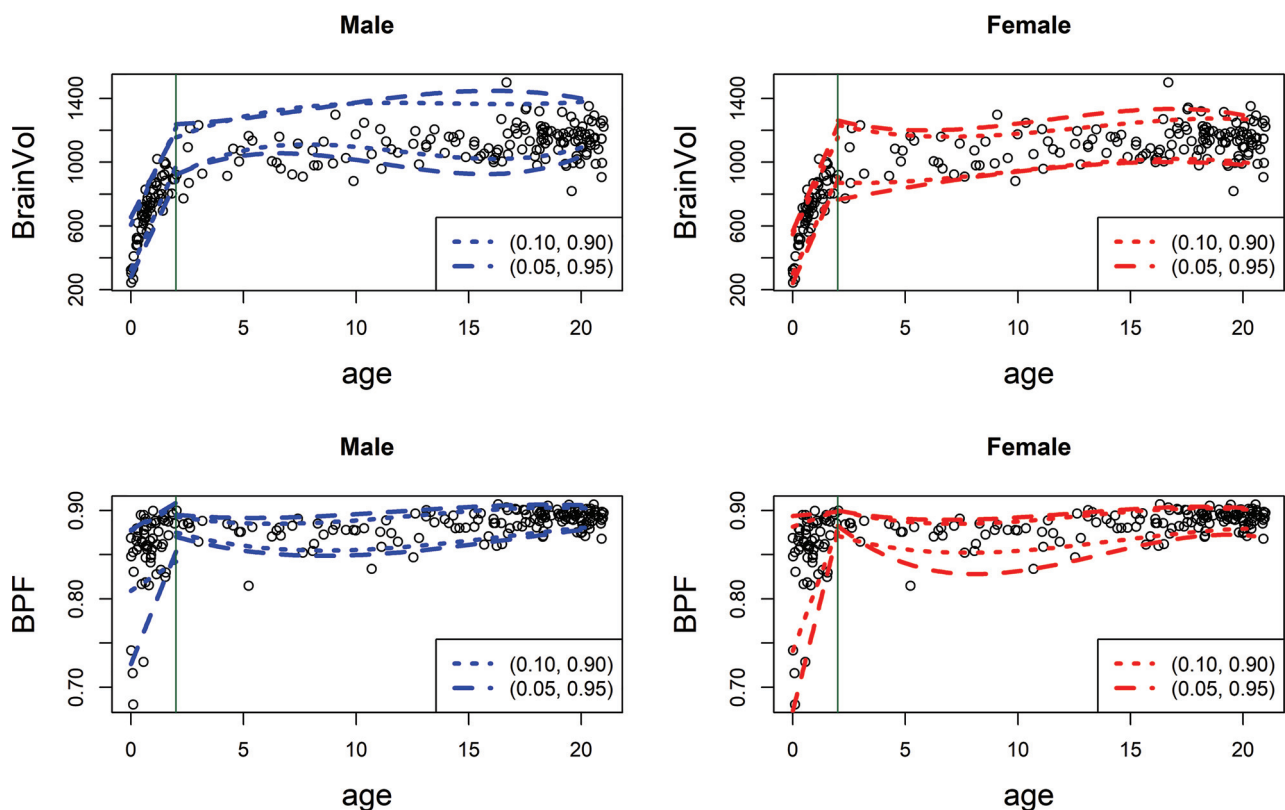


**FIG 4.** Quantile regression of brain volume (*upper graphs*) and BPF (*lower graphs*), male on the left, female on the right. The 5%–95% and 10%–90% quantiles are shown.

mean brain radiodensity is abnormal in hypoxic-ischemic encephalopathy following cardiac arrest, for example, and quantitative assessment appears to have diagnostic and prognostic implications.<sup>6-8</sup> It may be reasonable to expect that other forms of encephalopathy may also be abnormal with respect to radiodensity. We have found that global brain radiodensity is abnormal in multiple sclerosis,<sup>9</sup> and we have recently shown that mean brain radiodensity shows a statistically significant decline as a function of age in older adults.<sup>10</sup> Thus, radiodensity may also be abnormal in other neurodegenerative diseases or in congenital neurologic conditions. These are topics for future investigation.

At imaging, tissue volume is a surrogate for tissue mass or weight because it might be obtained at postmortem examination. Because mass is the product of volume-by-density, the truer correlate of weight is volume-by-radiodensity, or radiomass, though this correlate has received little attention in the literature. Because we have evidence that both measured brain volume and radiodensity may have clinical significance, radiomass is a valid topic for investigation. In multiple sclerosis, for example, both brain volume<sup>3,4</sup> and brain density<sup>9</sup> are abnormal, and both mean brain radiodensity and brain volume decline as a function of age.<sup>10</sup> Therefore the product of these measures may be abnormal in MS and potentially in other neurodegenerative diseases as well. This is a direction for future investigation.

### **Leveraging the Clinical Archive to Create a Reference Data Base for Head CT Imaging**

Because CT entails a radiation dose, limiting prospective human subject research, we propose to leverage the existing clinical image archive to generate a reference data base. An argument against the use of clinical images is that patients are not truly healthy because they have been scanned for a clinical indication. We contend that large data bases generated from clinical scans with structurally normal findings will approximate normalcy. Additionally, the data base generated from clinical images reflects the clinical spectrum of interest to physicians, rather than a data base of cases with truly normal findings. We support this argument by comparing it with published data on subjects with normal findings (largely generated by MR imaging) and demonstrating statistical integrity by showing that our results are internally consistent, with relatively few outliers, with very similar findings between male and female patients.

### **Brain Volume and BPF**

Regarding brain volume, we had previously shown that by means of clinical head CT data, brain volume increases from approximately 360 cm<sup>3</sup> to 1072 cm<sup>3</sup> at 2 years.<sup>11</sup> The current study shows a continued small increase in brain volume after 2 years of age, to reach a volume of 1350 cm<sup>3</sup> at 20 years of age, an approximately 3.8-fold increase in volume from birth to early adulthood. Also, consistent with published findings, male brains are consistently larger than female brains, not correcting for body size, and this difference is seen very early in development and reaches an approximately 10% difference by 20 years of age,<sup>14</sup> findings similar to those found at MR imaging.<sup>15</sup>

BPF is the ratio of the brain volume to the intracranial volume and has been widely used in the adult population as a means of measuring brain atrophy while normalizing for head size.<sup>16,17</sup> An MR imaging study by Bartholomew et al<sup>18</sup> investigated the BPF of children to find that the head circumference was an excellent predictor of brain volume in children 1.7 to 6 years of age. In further studies, BPF has been investigated in the preterm infant<sup>19</sup> and younger pediatric<sup>15</sup> populations using MR imaging, to find a wider range of normal CSF volumes occurring in children younger than 2 years of age. Our study also shows that the BPF is variable in the postnatal period and approaches adult values (0.85–0.90) at about 2 years of age, evidence that head circumference is a less accurate predictor of brain volume in this younger age group, similar to the findings reported for MR imaging.<sup>15</sup> This pattern may suggest that the BPF is more variable before the closure of the fontanelles, which typically occurs within the first 2 years of life.<sup>20</sup>

Because the brain volume continues to increase slightly through late adolescence and early adulthood, the BPF also continues to increase. The increase is statistically significant and not significantly different between the male and female cohorts (Table 2 and Fig 2B and Fig 3), as has been noted in an MR imaging study.<sup>15</sup> Using statistical modeling methods, we found that brain growth, both in volume and BPF, exhibited 2 distinct phases of growth as identified by 2D cluster analysis using a Gaussian mixture model (Online Fig 1) and is best modeled using a linear regression from 0–2 years of age and a polynomial equation after 2 years. Other models are possible. Although there are relatively few studies modeling total brain growth through the adolescent and early adult periods, there are none using CT scans. Others have also noted that the most significant volume changes occur in the first 2 years, with a more linear growth and a nonlinear, flattening trajectory thereafter.<sup>14,15,21</sup>

### **Radiodensity and Radiomass**

CT measures radiodensity, an intrinsic tissue property, and automated segmentation can readily yield a mean brain radiodensity assessment. We had previously shown that the radiodensity of brain tissue is lower at birth and rises to stable, near-adult values within the first year of life.<sup>11</sup> Here, we show that this small increase in brain radiodensity continues throughout adolescence.

As Hounsfield had observed, at CT imaging, x-ray absorbance and the associated signal intensity reflect mainly 1 variable—density, but also a minor one—atomic number.<sup>22</sup> When one compares like tissues of living persons, eg, the radiodensity values of the human brain, the contribution of differences in the mean atomic number is negligible, and the radiodensity is proportional to tissue density. We have found a strong correlation between the brain radiomass and the true brain weight as deduced from published postmortem examination values (data not shown). Published postmortem data show increasing brain weights throughout adolescence and early adulthood, with a peak brain weight reached at approximately 20 years of age.<sup>23</sup> These data evidence a brain weight of 369 g at birth and approximately 1300 g at 20 years of age. This 3.5-fold increase

in weight closely parallels the increase in brain radiomass observed in this study (3.8-fold).

### Quantile Regression

Quantile regression provides a means of quantitatively comparing an individual measure with its reference data base and a means of putting a given metric into a statistical context. Using quantile regression, a study outcome is not judged to be “normal” or “abnormal” but rather “at the nth percentile for age and sex.” While an extreme percentile measure may be used to trigger or validate further clinical inquiry, all studies would have associated quantitative metrics that can be followed across time in the event of repeat imaging.

### Study Limitations

For the current study, cases of patients older than 2 years of age were obtained from a single (LightSpeed VCT) CT scanner because we wished to investigate the variation among individuals as measured with a current standard clinical machine. Specifically, we wished to learn the variance among individuals in terms of brain volumes, BPF, and mean brain radiodensity and whether the variance was large enough to be detected with confidence above the variation in measure that can occur from a single, typical clinical scanner. Learning the answer to this question is an important first step in the investigation of the clinical use of quantitative CT.

We know from the literature that Hounsfield unit measures can vary with scan manufacturer,<sup>24</sup> with kilovolt (peak),<sup>24,25</sup> and probably with scan protocol. The contribution of these factors as they affect the Hounsfield unit measure of human brain is a topic for future investigation. In an earlier study of mean brain radiodensity, we compared the results from 3 different clinical machines to find small differences in scan values, but the overall pattern of mean brain Hounsfield unit changes as a function of age from all 3 machines was very similar.<sup>11</sup> A universal reference data base likely represents a future goal that may be achievable through higher calibration standards or statistical normalization of datasets.

### CONCLUSIONS

Clinical head CT images can be analyzed using automated segmentation algorithms to yield objective, reproducible, quantitative information about the pediatric brain. The existing clinical archive can be leveraged by processing previously acquired image datasets to generate reference data bases. Statistical methods such as quantile regression can be applied to a reference data base to compare individual patients with their age- and sex-matched peer group. These methods would facilitate quantitative reporting and have the potential to aid in the identification of pathology, though further research is needed.

### REFERENCES

1. Fjell AM, McEvoy L, Holland D, et al; Alzheimer's Disease Neuroimaging Initiative. **Brain changes in older adults at very low risk for Alzheimer's disease.** *J Neurosci* 2013;33:8237–42 [CrossRef Medline](#)
2. Rajagopalan V, Pioro EP. **Brain parenchymal fraction: a relatively simple MRI measure to clinically distinguish ALS phenotypes.** *Biomed Res Int* 2015;2015:693206 [CrossRef Medline](#)
3. Losseff NA, Wang L, Lai HM, et al. **Progressive cerebral atrophy in multiple sclerosis: a serial MRI study.** *Brain* 1996;119:2009–19 [CrossRef Medline](#)
4. Simon JH, Jacobs LD, Campion MK, et al. **A longitudinal study of brain atrophy in relapsing multiple sclerosis: the Multiple Sclerosis Collaborative Research Group (MSCRG).** *Neurology* 1999;53:139–48 [CrossRef Medline](#)
5. Adduru V, Baum SA, Zhang C, et al. **A method to estimate brain volume from head CT images and application to detect brain atrophy in Alzheimer disease.** *AJNR Am J Neuroradiol* 2020;41:224–30 [CrossRef Medline](#)
6. Choi SP, Park HK, Park KN, et al. **The density ratio of grey to white matter on computed tomography as an early predictor of vegetative state or death after cardiac arrest.** *Emerg Med J* 2008;25:666–69 [CrossRef Medline](#)
7. Lee BK, Jeung KW, Song KH, et al; Korean Hypothermia Network Investigators. **Prognostic values of gray matter to white matter ratios on early brain computed tomography in adult comatose patients after out-of-hospital cardiac arrest of cardiac etiology.** *Resuscitation* 2015;96:46–52 [CrossRef Medline](#)
8. Torbey MT, Selim M, Knorr J, et al. **Quantitative analysis of the loss of distinction between gray and white matter in comatose patients after cardiac arrest.** *Stroke* 2000;31:2163–67 [CrossRef Medline](#)
9. Cauley KA, Fielden SW. **A radiodensity histogram study of the brain in multiple sclerosis.** *Tomography* 2018;4:194–203 [CrossRef Medline](#)
10. Cauley KA, Hu Y, Fielden SW. **Aging and the brain: a quantitative study of clinical CT images.** *AJNR Am J Neuroradiol* 2020;41:809–14 [CrossRef Medline](#)
11. Cauley KA, Hu Y, Och J, et al. **Modeling early postnatal brain growth and development with CT: changes in the brain radiodensity histogram from birth to 2 years.** *AJNR Am J Neuroradiol* 2018;39:775–81 [CrossRef Medline](#)
12. Jenkinson M, Beckmann CF, Behrens TE, et al. **FSL.** *Neuroimage* 2012;62:782–90 [CrossRef Medline](#)
13. Muschelli J, Ullman NL, Mould WA, et al. **Validated automatic brain extraction of head CT images.** *Neuroimage* 2015;114:379–85 [CrossRef Medline](#)
14. Courchesne E, Chisum HJ, Townsend J, et al. **Normal brain development and aging: quantitative analysis at in vivo MR imaging in healthy volunteers.** *Radiology* 2000;216:672–82 [CrossRef Medline](#)
15. McAllister A, Leach J, West H, et al. **Quantitative synthetic MRI in children: normative intracranial tissue segmentation values during development.** *AJNR Am J Neuroradiol* 2017;38:2364–72 [CrossRef Medline](#)
16. Rudick RA, Fisher E, Lee JC, et al. **Use of the brain parenchymal fraction to measure whole brain atrophy in relapsing-remitting MS: Multiple Sclerosis Collaborative Research Group.** *Neurology* 1999;53:1698–1704 [CrossRef Medline](#)
17. Vagberg M, Granasen G, Svenningsson A. **Brain parenchymal fraction in healthy adults: a systematic review of the literature.** *PLoS One* 2017;12:e0170018 [CrossRef Medline](#)
18. Bartholomeusz HH, Courchesne E, Karns CM. **Relationship between head circumference and brain volume in healthy normal toddlers, children, and adults.** *Neuropediatrics* 2002;33:239–41 [CrossRef Medline](#)
19. Vanderhasselt T, Naeyaert M, Watte N, et al. **Synthetic MRI of preterm infants at term-equivalent age: evaluation of diagnostic image quality and automated brain volume segmentation.** *AJNR Am J Neuroradiol* 2020;41:882–88 [CrossRef Medline](#)
20. Aisenson MR. **Closing of the anterior fontanelle.** *Pediatrics* 1950;6:223–26 [Medline](#)

21. Zhang L, Thomas KM, Davidson MC, et al. **MR quantitation of volume and diffusion changes in the developing brain.** *AJNR Am J Neuroradiol* 2005;26:45–49 [Medline](#)
22. Hounsfield GN. **Computed medical imaging.** Nobel lecture, December 8, 1979. *J Comput Assist Tomogr* 1980;4:665–64 [CrossRef](#) [Medline](#)
23. Dekaban AS. **Changes in brain weights during the span of human life: relation of brain weights to body heights and body weights.** *Ann Neurol* 1978;4:345–56 [CrossRef](#) [Medline](#)
24. Cropp RJ, Seslija P, Tso D, et al. **Scanner and kVp dependence of measured CT numbers in the ACR CT phantom.** *J Appl Clin Med Phys* 2013;14:4417 [CrossRef](#) [Medline](#)
25. Pomerantz SR, Kamalian S, Zhang D, et al. **Virtual monochromatic reconstruction of dual-energy unenhanced head CT at 65-75 keV maximizes image quality compared with conventional polychromatic CT.** *Radiology* 2013;266:318–25 [CrossRef](#) [Medline](#)